Comparative Analysis of IR and Vibrational Circular Dichroism Spectra for a Series of Camphor-Related Molecules

Sergio Abbate,*[,†,‡] Luigi Filippo Burgi,[†] Fabrizio Gangemi,[†,‡] Roberto Gangemi,[†,‡] France Lebon,[†,‡] Giovanna Longhi,[†,‡] Vaughan M. Pultz,[§] and David A. Lightner[||]

Dipartimento di Scienze Biomediche e Biotecnologie, Università di Brescia, Viale Europa 11, 25123 Brescia, Italy, Consorzio Interuniversitario per le Scienze Fisiche della Materia, CNISM, via della Vasca Navale, 84, 00146, Roma, Italy, Department of Chemistry, Truman State University, Kirksville, Missouri 63501, and Department of Chemistry, University of Nevada, Reno, Nevada 89557

Received: June 16, 2009; Revised Manuscript Received: September 9, 2009

The absorption spectra and vibrational circular dichroism (VCD) spectra in the mid-IR range 1600−950 cm^{-1} of 10 camphor-related compounds have been recorded and compared to DFT calculated spectra at the B3PW91/TZ2P level and have been examined together with the corresponding data of the parent molecules. The rigidity of the bridged structure common to all compounds investigated permits (a) identification of three spectroscopic regions in the mid-IR range that can be "used" separately by the interested stereochemist for structural diagnosis and assignment of some major characteristics of the VCD spectra in these regions to what we call "skeletal chiral sense" and (b) recognition of possible conformers for flexible substituent groups, when present. VCD spectra of the 10 molecules have been recorded and analyzed also in the CH-stretching region, 3100−2800 cm^{-1}. Here, we have been able to identify and characterize features of vibrational excitons by comparison of data within the 10-molecule class. To find a theoretical justification of result (a), we have examined the potential energy distribution of the normal modes in the mid-IR range, the partitioning of the calculated rotational strengths in terms of contributions from all couples of internal coordinates, the angle formed by the two vectors, the electric dipole transition moment and the magnetic dipole transition moment, and finally the overlap of normal modes of different molecules. A discussion is provided as to the usability of the introduced algorithms.

1. Introduction

Bicyclic ketones have been investigated quite extensively through electronic circular dichroism (CD) spectroscopy and have allowed verification of the octant rule and definition of the nodal planes or characterization of antioctant behavior.[1] More recently, they have proven useful to test ab initio and DFT calculations.[2,3] Finally, these systems have also proved quite useful for advancing the field of vibrational circular dichroism (VCD).[4−6] We have recently contributed to this area by analyzing and comparing the infrared (IR) and VCD spectra of camphor, fenchone, and their corresponding 2-olefinic derivatives.[7] The present work is a continuation and completion of studies in ref 7, and we will focus on several camphor-related molecules of two types. The first type is where the group at C(1) is changed ad hoc, or the oxygen atom O at C(2) is substituted by sulfur S (first line of Scheme 1); the second group is comprised of molecules with larger differences from camphor, that is, with either large substituent groups at C(2) or C(3) (compounds **8**, **9**, and **10** of Scheme 1) or with the C5−C6 moiety altered (compounds **6** and **7** of Scheme 1). Although VCD data for camphor itself are present in the literature, they are represented here, on the basis of our own experiments and calculations, for continuity and discussion.

IR and VCD studies in the so-called mid-IR range (950−1600 cm^{-1}) of molecules like those shown in Scheme 1 provide regions containing quite diverse information, with some regions being underrepresented and sparse in useful data, yet others instead containing large amounts of either configurational or conformational information. Some regions contain IR (or VCD) intense bands; others contain only weak IR (or VCD) bands. The aim of this work is then 3-fold:

(a) The first is to obtain the definition and analysis of three regions within the 950−1600 cm^{-1} range that exhibit similar behavior, and correspond to the presence of given moieties in all of the molecules, or that, on the contrary, change markedly upon substitution of those groups. Comparison of the data for **1**−**5** especially will serve this scope, because the substituent groups do not introduce conformational degrees of freedom, and consequently we expect the appearance of the IR and VCD spectra to change slightly and in well-defined regions. More important changes in given spectroscopic regions are expected for molecules **6**−**10**, but still the changes should be rationalized starting from the VCD data of **1**. Indeed, we will try first to define which spectroscopic features are associated with the bridged structure and which ones are associated with the substituent groups. We will also discuss whether dividing the two types of moieties has some more fundamental justification. To this end, we have examined the potential energy distribution of the calculated normal modes in the mid-IR range, and we have built a partitioning of the corresponding rotational strengths in terms of contributions from all couples of internal coordinates.[8−10] Furthermore, the recently introduced analysis

* Corresponding author. Tel.: +39 030 3717415. Fax: +39 030 3717415. E-mail: abbate@med.unibs.it.
[†] Università di Brescia.
[‡] CNISM.
[§] Truman State University.
[||] University of Nevada.

10.1021/jp905644d CCC: $40.75
Published on Web 09/29/2009

SCHEME 1

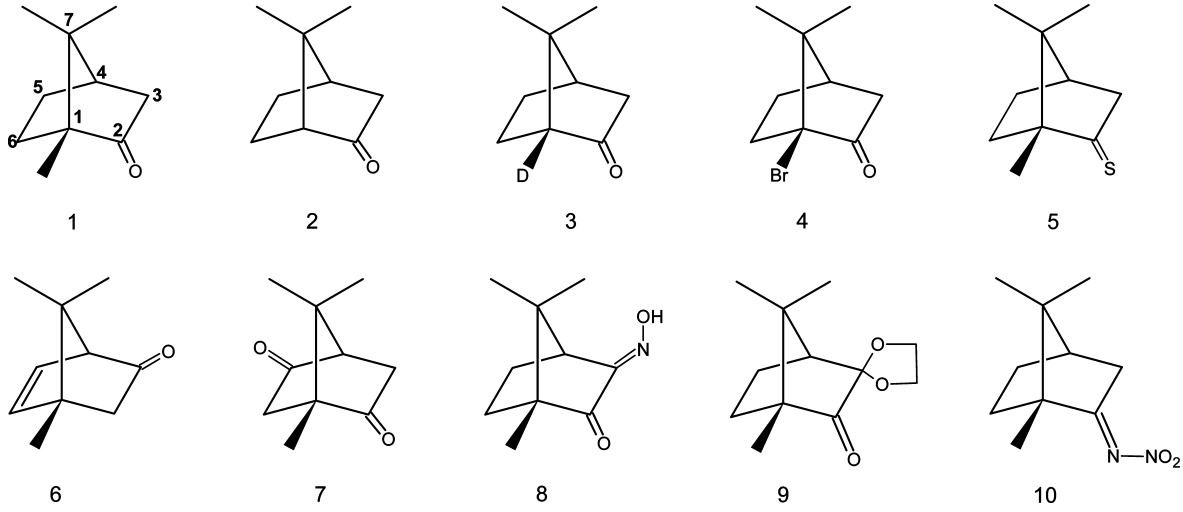

of normal modes robustness and normal mode overlap in related molecules will be considered.[11]

(b) The rotameric states of the substituent groups in either position 2 or 3 for compounds **8**−**10** are expected to provide specific signals in the IR and VCD spectra, much in a way similar to what has been evidenced for the rotameric states of borneol and borneol related molecules.[12] Recently, other types of spectroscopic manifestations of mobile groups were pointed out,[13,14] and we will seek whether they are present also here.

(c) Finally, we analyze the CH-stretching region and find a few "excitonic" type CH-stretching VCD bands[15] for camphor-based molecules, particularly for antisymmetric normal modes.

2. Materials and Methods

Synthesis. VCD data of compound **1** have been analyzed in several papers in the literature, and we report here the results from previous work of our group. Compound **5**, in the (1*R*)-(−) enantiomeric form, was purchased from Sigma-Aldrich and used without further purification. Compound **8** was also from Sigma-Aldrich; more precisely, we purchased (1R)-(+)-camphorquinone-3*E*-oxime 99% and (1*S*)-(−)-camphorquinone-3*E*-oxime 99%. (For the definition of the absolute configuration, see also the 1994 Fluka catalog, together with a list of references therein discussing the preparation procedure.) As for the *E*-configuration of the C═N-bond, IR spectroscopy on very dilute solutions (≤0.005 M/CCl_4) confirms that the compound is *E* and not *Z*. All of the remaining compounds were synthesized at the University of Nevada and have been reported in the literature. (In ref 16, we report a synopsis of references for all compounds **1**−**10**.) Except **4** and **6**, all of them were obtained as single (1*R*)-enantiomers, and also **10** was in the *E* form.

IR and IR-VCD Spectra Measurements. IR absorption spectra, IR spectra for short, and IR-VCD spectra were recorded with a JASCO FVS4000 FTIR spectropolarimeter equipped with two detectors, an MCT and an InSb. The first one has been used to investigate the mid-IR region, 900−1600 cm^{-1}. The second one is for the CH-stretching region, 2800−3100 cm^{-1}; for the former region, 2000 scans were needed for each spectrum at 4 cm^{-1} resolution (∼20 min), and for the latter one 10 000 scans were needed at 8 cm^{-1} resolution (∼1.2 h). However, due to limited sample availability for compounds **2**, **3**, and **4**, we prefer to use the data in the range 2800−3100 cm^{-1} taken some time ago at the Chemistry Department of the University of Minnesota on a dispersive noncommercial apparatus. Spectra were recorded for CCl_4 solutions for **1**−**4** and for $CDCl_3$ solutions for **5**−**10**. Concentrations ranged from 0.08 to 1.2 M, making sure that absorbance maxima were below 1 at all times; BaF_2 cells with path lengths 50−100 μm were used. The IR spectra reported below were obtained by subtracting out the IR spectra of the solvent; also, the VCD spectra were obtained by subtracting the baseline obtained recording the VCD data on the solvent. Besides, because for compounds **1** and **8** both enantiomers were available, the reported VCD spectra in this case are the half difference of the VCD spectra of the two enantiomers; for the (*R*)-enantiomer, we report the VCD spectrum obtained as (1/2)[(*R*) − (*S*)]. (Of course, in these cases we verify first that mirror image spectra are obtained for the two enantiomers).

Density Functional Theory (DFT) Calculations. The method employed here to calculate dipole and rotational strengths is the one elaborated in a number of papers,[17] especially by Stephens and collaborators, and has been amply used in the VCD literature. This method is implemented in the DFT approach and allows one to assign the VCD spectra in the mid-IR easily. Using the Gaussian 03/GAUSSVIEW suite of programs,[18] calculations were run with either B3LYP and B3PW91 functionals and with 6-31G** and TZ2P bases: the latter basis set is built from the Huzinaga−Dunning TZ set, with the addition of two sets of polarization functions from Dunning's cc-pVTZ, as available from the Internet.[19] The results in most cases are similar, and thus we report the data on the basis of the B3PW91/TZ2P choice; from calculated harmonic frequencies, dipole, and rotational strengths, we have generated a calculated IR and VCD spectrum for each molecule, by assigning a Lorentzian band shape to each fundamental vibrational transition. We have done so by using a routine in the JASCO FVS4000 software with $\gamma = 8$ cm^{-1} (for the mid-IR region) and $\gamma = 16$ cm^{-1} (for the CH-stretching region); in all cases, a frequency scaling factor of 0.975 has been adopted, to facilitate comparison of calculated and experimental spectra (this factor is optimal for features with $\nu \approx 1200$ cm^{-1}). We can state that the alternative choice presented just above for functional/basis set gives good results in all cases considered here. For the sulfur atom, we adopted Ahlrichs' TZV set, with the addition of two sets of polarization functions from Dunning's cc-pVTZ, and for bromine, simply Ahlrichs' TZV set.[19]

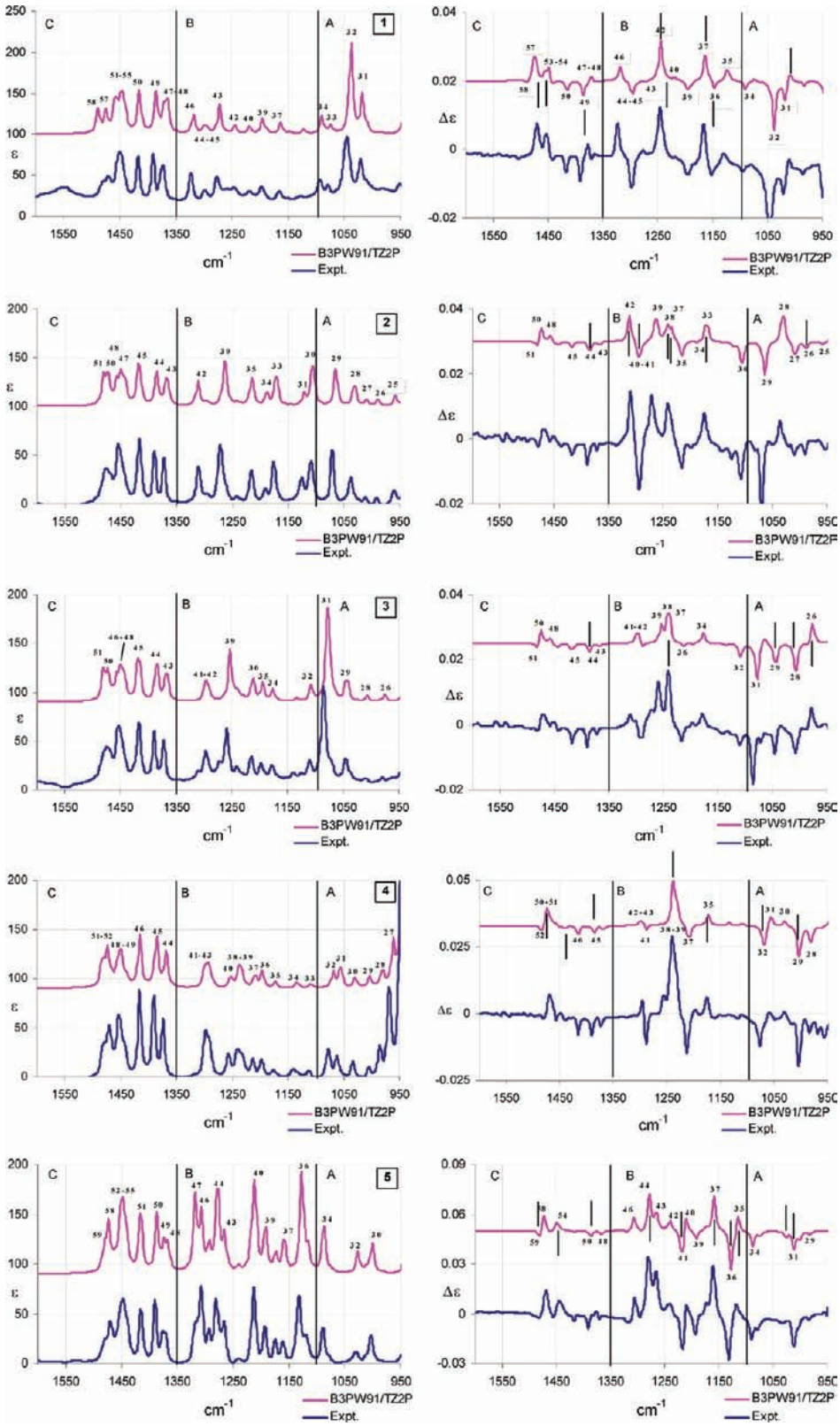

Figure 1. Experimental and calculated IR absorption (left) and VCD (right) spectra in the mid-IR region for molecules **1**−**5** of Scheme 1. In all graphs, ε and $\Delta\varepsilon$ are in 10^3 cm^2 mol^{-1} units. Vertical black bars designate modes in the top class of robustness (r*).

3. Results and Discussion

The best accessible regions to our instrumentation and the only ones studied here cover two ranges: the mid-IR region (950−1600 cm^{-1}) and the CH-stretching region (2800−3100 cm^{-1}). In relation to points (a) and (b) addressed in the Introduction, we will first analyze the mid-IR region, which is also the most studied in the literature. As indicated in Scheme 1, the results reported in the following refer all to the (*R*) configuration for asymmetric carbon atom #1, except for **4** and **6**.

The Mid-IR Region (1600−950 cm^{-1}). ***a. Partitioning of Spectroscopic Regions.*** For sake of discussion, we partition our results as follows: in Figure 1, we compare experimental and

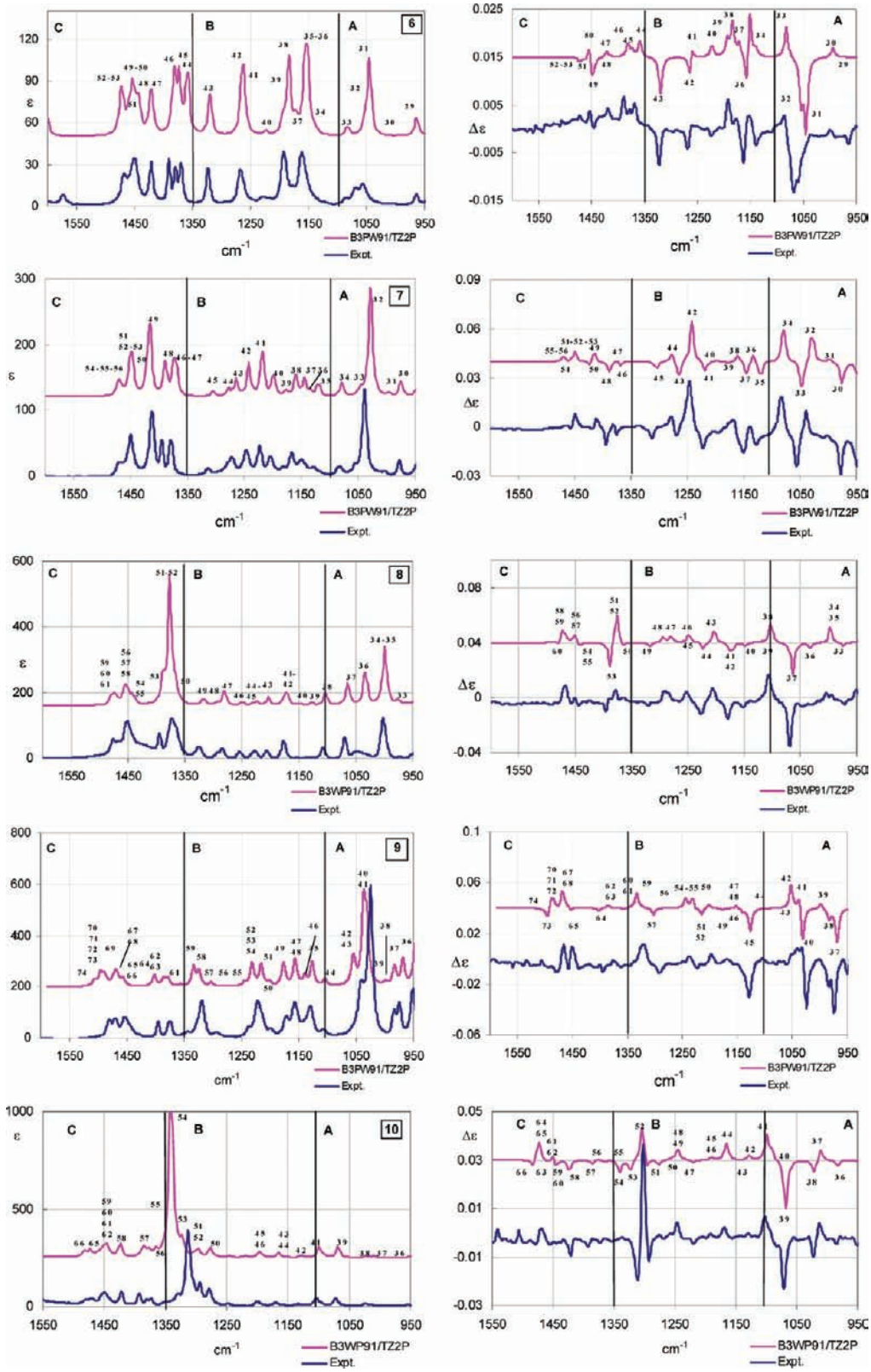

Figure 2. Experimental and calculated IR absorption (left) and VCD (right) spectra in the mid-IR region for molecules **6**−**10** in Scheme 1. In all graphs, ε and $\Delta\varepsilon$ are in 10^3 cm^2 mol^{-1} units.

calculated IR and VCD spectra for compounds **1**−**5**; in Figure 2, we compare experimental and calculated IR and VCD spectra for compounds **6**−**10**. The numbers reported close to the calculated features are the normal mode (NM) numbers from 1 to $3N - 6$, as calculated in the normal mode analysis by Gaussian 03; the lowest numbers correspond to the lowest frequencies, and there is only an approximate correspondence among numbers in different molecules. However, they facilitate comparison of spectra for the different compounds and are useful in examining the tables below. As expected for these compounds, the agreement of calculated and experimental IR and VCD spectra is quite good (some exception is noticed in **10** for the intense doublet at ∼1313−1304 cm^{-1}); however, the scope here is not to establish absolute configuration, which is under

TABLE 1: Calculated Frequencies ω (cm^{-1}), Dipole Strengths (10^{-40} esu^2 cm^2), Rotational Strengths (10^{-44} esu^2 cm^2), and Potential Energy Distribution (PED) in Percentage for (*1R*)-Camphor (1) for the Normal Modes from #24 to #59[a]

	NM#	ω	D	R		%		%		%		%		%		%
A	24	926	4.4	−12.2	trigd	20	Zrock'	13	C1C6	9	3rock	7	sydbrid4	6	C4C7	6
	25	941	8.6	26.3	3rock	25	6rock	13	C3C4	8	5rock	7	5twist	6	xrock'	6
	26	952	10.8	12.7	C5C6	19	C7CY	16	Xrock	11	C7CX	9	C3C4	5	Yrock	5
	27	958	4.0	−2.7	Yrock'	24	xrock'	23	Xrock	11	Yrock	11	C7CX	10	C7CY	8
	28	968	13.5	−11.2	C5C6	21	C7CX	10	Yrock	9	C3C4	7	xrock'	7	C7CY	6
	29	1004	1.5	−3.6	Yrock	20	Xrock	19	Yrock'	12	C5C6	10	C4C5	9	C3C4	7
	30	1030	3.6	7.8	Zrock	14	Xrock	13	C4C5	8	C3C4	8	4rock'	7	Yrock	6
	31	1040	52.0	−15.6	3rock	12	4rock	11	Zrock	8	5rock	8	C4C5	8	C2C3	7
	32	1061	116.8	−38.1	C2C3	19	6twist	11	ipCO	11	trigd	7	C1C2	7	4rock'	6
	33	1098	9.9	1.8	3twist	25	5twist	11	4rock'	8	Zrock	8	6twist	7	5rock	5
B	34	1115	21.9	−6.0	Zrock'	15	xrock'	10	4rock	10	Yrock'	8	5twist	5	Zrock	5
	35	1149	5.1	9.0	3twist	16	C1C6	10	Zrock'	10	Zrock	8	C7CY	8	C7CX	8
	36	1173	2.0	−6.4	6rock	9	Zrock'	8	5rock	6	Yrock	6	C7CX	6	C1C7	5
	37	1190	13.0	19.8	CZC1	14	4rock	13	3twist	13	6twist	9	Xrock	7	5twist	7
	38	1217	2.5	−2.5	6wag	14	4rock'	9	3wag	8	CZC1	7	C3C4	5		
	39	1224	16.3	−5.1	4rock	13	6twist	13	Yrock	11	3twist	9	C7CX	8	Xrock	7
	40	1248	7.5	2.0	6wag	21	5twist	17	C7CY	11	xrock'	9	C1C7	5		
	41	1268	0.3	2.8	3wag	40	5wag	11	C3C4	10	5twist	7				
	42	1275	8.6	26.3	6twist	28	5twist	11	7rock	7	6wag	5	C7CY	5	3twist	5
	43	1303	32.7	−1.1	5wag	14	C4C5	8	3wag	8	4rock'	7	4rock	5	asdrin	5
	44	1327	4.9	−7.2	4rock'	37	4rock	10	5twist	8	3wag	7	C3C4	5		
	45	1332	6.3	−3.4	5wag	52	4rock'	12	4rock	9						
	46	1352	19.6	9.2	6wag	34	CZC1	14	C1C2	6	sydbrid1	5	C1C7	5		
C	47	1400	27.1	−1.0	Xsymd	61	Ysymd	27	C7CX	6						
	48	1406	21.2	3.8	Zsymd	78	CZC1	12	Ysymd	5						
	49	1421	39.1	−9.0	Ysymd	56	Xsymd	26	Zsymd	7						
	50	1452	40.6	−5.1	3sc	86										
	51	1479	10.4	−1.7	Xasyd'	26	6sc	15	Yasyd'	15	Xasyd	14	Zasyd	12	Yasyd	9
	52	1482	21.4	−2.2	Zasyd	49	Yasyd'	14	Xasyd'	14	Xasyd	7				
	53	1487	21.5	7.4	Zasyd'	42	Yasyd	20	Xasyd	11	Xasyd'	7				
	54	1494	15.9	3.6	Zasyd'	35	Xasyd	17	6sc	13	5sc	11	Zasyd	7	Yasyd'	7
	55	1498	18.2	−0.5	Yasyd'	31	6sc	19	Xasyd	19	Zasyd	16				
	56	1510	1.7	1.4	Yasyd	53	Xasyd	15	5sc	8	Zasyd'	7	Yrock'	5		
	57	1514	18.2	14.1	6sc	42	Xasyd'	31	Yasyd'	14						
	58	1529	21.7	−1.5	5sc	65	Xasyd'	9	6sc	9	Xasyd	6				
	59	1821	555.7	18.0	C2O	88										

[a] For the definition of group coordinates, see Table 3. The qualitative regions A, B, and C are also defined in the first column (see text).

no doubt, but rather to devise simple observations for handy use in analyzing similar bicyclic structural models. For this reason and bearing in mind goal (a) of this work, we have divided all of the spectra of the figures into three ranges, which we discuss separately: the 950−1100 cm^{-1} range (A in the figures), the 1100−1350 cm^{-1} range (B in the figures), and the 1350−1600 cm^{-1} range (C in the figures).

I. Region between 950 and 1100 cm^{-1} (Range A). The spectra are here limited to 950 cm^{-1}, due to the use of $CDCl_3$ as solvent. Two facts are worth commenting:

IR. Looking at Figure 1, one concludes that the IR bands are generally all pretty intense and the IR spectrum is dominated by the band at 1047 cm^{-1} for compounds **1** (corresponding to NM #32), **2** (NM #29), and **3** (NM #31), reaching ε values close to 100×10^3 cm^2/mol; for **4** and **5**, this band is weaker (in **4** a very strong band is observed at 970 cm^{-1}). The same observation holds true also for the IR spectra of Figure 2, with the sole exception of compound **6**, and with a band of compound **9** boosting to $\varepsilon = 500 \times 10^3$ cm^2/mol that, by the methods illustrated below, is attributed to vibrational modes of the external ring in position 2.

From normal mode (NM) and potential energy distribution (PED) analysis (vide infra), we will see that mixed modes contribute to this region, which comprise: CH-deformations (mainly rocking), CC-stretchings, and the in-plane bending of the carbonyl group. In particular, the 1045−1080 cm^{-1} band for **1**−**3** and **6**,**7** is due to stretchings of CC bonds in the vicinity of the carbonyl group, corresponding to NM #32 in **1** and the similar mode in the other molecules. When the C═O group is not present, as in the 2-olefinic derivative of camphor,[7] the whole region A is less intense. Also, when the C═O is substituted, as in compounds **5** and **10**, the normal mode #32 (or similar) band and the whole region are less intense. The presence in compound **4** of a bromine atom in position 2 in place of a methyl also causes a decrease of intensity of NM #32.

VCD. The VCD spectra are quite intense for **1**−**5**, reaching $\Delta\varepsilon_{max} \approx -0.02 \times 10^3$ cm^2/mol (corresponding to NM #32 or the similar mode), and are even more intense for **8**−**10** where a negative band has a $\Delta\varepsilon$ value close to -0.04×10^3 cm^2/mol. The sum of rotational strengths is negative for all compounds, and this overall negative VCD correlates to the molecular shape of the bicyclic skeleton with respect to the carbonyl (or CX) group in position 2, which is the same for all molecules **1** to **10** (except **6** as commented below). The discriminating factor is an "absolute shape", that is, the absolute stereochemical sense of the bicyclic skeleton with respect to the substituent in position 2, instead of the absolute configuration of the asymmetric carbon 4 or 1, which can be (*R*) or (*S*). A Br- or an H- or a D-atom or a methyl group in position 1 does not make a difference in the stereochemical shape of the bicyclic skeleton and does not alter much the rings' vibrational modes and VCD, but it is crucial in the Cahn−Ingold−Prelog definition of the absolute configuration of **4**. In the case of compound **6**, the bicyclic stereochemical sense with respect to the carbonyl is a mirror image

TABLE 2: Calculated Frequencies ω (cm^{-1}), Dipole Strengths (10^{-40} esu^2 cm^2), Rotational Strengths (10^{-44} esu^2 cm^2), and Potential Energy Distribution (PED) in Percentage for (1*R*)-Thiocamphor (5) for the Normal Modes from #24 to #59[a]

	NM#	ω	*D*	*R*		%		%		%		%		%		%
A	24	922	10.7	−48.1	3rock	20	Trigd	14	Zrock'	10	C5C6	8	C1C6	7	asdrin'	5
	25	934	8.0	29.5	3rock	18	6rock	12	C3C4	11	Zrock	7	5twist	7	xrock'	5
	26	955	14.0	6.5	C5C6	16	C7CY	15	C7CX	11	Xrock	9	Yrock	7	C4C7	5
	27	960	1.1	−4.5	xrock'	31	Yrock'	20	C7CY	14	Xrock	8				
	28	964	15.8	−0.2	C5C6	19	C7CX	15	Yrock	13	Yrock'	9	C3C4	6		
	29	1003	1.4	−5.7	Yrock	20	Xrock	17	Yrock'	10	C5C6	9	C4C5	7	C3C4	7
	30	1022	34.4	−11.0	Zrock	24	Xrock	15	4rock	8	C2C3	7	5rock	5	xrock'	5
	31	1033	4.8	−29.1	C4C5	20	3rock	10	C5C6	10	Yrock	7	3twist	7	C3C4	6
	32	1048	23.0	−8.4	C2C3	23	6twist	12	C1C2	9	5rock	8	trigd	7	6rock	5
	33	1098	3.0	−6.1	5twist	16	3twist	16	Zrock	14	6twist	10	4rock'	9	5rock	6
B	34	1112	47.9	−23.9	Zrock'	20	3twist	13	4rock	10	Yrock'	9	xrock'	8	5wag	7
	35	1140	22.3	26.8	3twist	19	Zrock'	16	C1C6	11	3wag	5	4rock	5	Zrock	5
	36	1153	98.9	−62.3	C2S	11	5twist	10	6rock	9	C7CX	8	Zrock	7	C7CY	7
	37	1185	30.2	51.8	3twist	17	CZC1	16	6twist	8	Xrock	5	C4C7	5	Yrock	5
	38	1201	16.2	3.5	3wag	17	4rock'	7	C7CY	7	C2S	6	Zrock'	6	C3C4	5
	39	1220	38.1	−11.9	4rock	17	6twist	11	Yrock	8	C7CX	8	7sc	5	3twist	5
	40	1240	78.8	26.2	6wag	22	3wag	12	CZC1	8	C2S	7	trigd	7	7wag	7
	41	1247	20.2	−35.9	5twist	30	C7CY	13	xrock'	7	7sc	5				
	42	1270	4.3	13.5	6twist	29	5twist	8	7rock	7	6wag	7	C7CX	6	C7CY	5
	43	1296	31.1	20.0	5wag	24	C4C5	12	4rock'	10	C1C2	7	3twist	5		
	44	1309	71.8	48.8	4rock	12	C2S	9	5twist	9	C3C4	8	C7CX	6	C4C7	6
	45	1325	19.4	−4.5	4rock'	34	5wag	28	6wag	6	3wag	5				
	46	1340	47.6	17.4	5wag	16	4rock	14	3wag	12	6wag	11	C2C3	5		
	47	1351	62.3	−3.5	6wag	22	3wag	17	C2S	13	C1C2	12	CZC1	7		
C	48	1402	20.3	−3.7	Ysymd	57	Xsymd	31	C7CY	5						
	49	1410	20.4	0.2	Zsymd	76	CZC1	11	Xsymd	5						
	50	1422	46.3	−5.8	Xsymd	52	Ysymd	28	Zsymd	8						
	51	1453	44.3	−1.5	3sc	83	Yasyd'	5								
	52	1477	12.9	−0.1	Zasyd	21	6sc	20	Xasyd'	17	Xasyd	15	Yasyd	10	Yasyd'	6
	53	1482	21.7	1.9	Zasyd	46	Yasyd'	15	Xasyd'	15	Zasyd'	7	Zrock'	5		
	54	1487	38.2	8.8	Zasyd'	37	Yasyd	21	Xasyd'	11	Xasyd	10	5sc	9		
	55	1491	18.7	0.7	Zasyd'	26	6sc	21	5sc	18	Yasyd'	17	Yasyd	6		
	56	1501	7.6	−3.0	Xasyd	28	Zasyd	20	Yasyd'	18	Zasyd'	10	6sc	7		
	57	1508	2.9	0.4	Yasyd	39	5sc	25	Xasyd	15	Xasyd'	6				
	58	1513	34.7	19.7	6sc	42	Xasyd'	23	Yasyd'	15	5sc	7				
	59	1521	17.1	−10.2	5sc	31	Xasyd'	15	Yasyd'	13	Xasyd	13	Yasyd	9	6sc	6

[a] For the definition of group coordinates, see Table 3. The qualitative regions A, B, and C are also defined in the first column (see text).

of camphor; for this reason, one should expect an opposite behavior; however, in this case the presence of olefinic CH influences the spectrum with a negative band at 1070 cm^{-1} (#31 calculated at 1077 cm^{-1}) due to in-plane bendings.

To check whether the bicyclic skeletal sense with respect to the carbonyl in **2** dictates the prevalent sign of this spectral region, we considered the VCD spectrum of epicamphor, as calculated with the same functional and basis set (see the Supporting Information). Indeed, the calculated VCD spectrum for (1*S*,4*S*)-epicamphor presents many bands with opposite sign with respect to those of (1*R*,4*R*)-camphor, because the two molecules are mirror images of each other apart from the methyl of carbon 1 in camphor and carbon 4 in epicamphor. However, in epicamphor, vibrational modes involving the methine and the methylene groups contiguous to the carbonyl originate a strong conservative (−,+) couplet, calculated at 1101 and 1142 cm^{-1}, not present in camphor.

Why the VCD spectrum of region A is nonconservative and adds up to a negative value will be discussed below, and evidence will be sought on whether vibrational contributions of local symmetry coordinates contribute also to other spectroscopic regions. The VCD spectra of **1**, **2**, and **3** are quite similar, meaning that the difference in substituent groups at position 1 has scarce influence on the overall aspect of this region. To a minor extent, this is true for **4**. For compound **7**, where a second C═O is present on the opposite side of the molecule, the overall negative aspect of VCD is less certain: among the observed features, one may recognize the (+,−) couplet calculated at 1078 and 1119 cm^{-1} (after scaling) for (1*R*,4*R*)-epicamphor (see the Supporting Information). The presence of electron-rich groups in position 3 is observed to increase the negative VCD, while maintaining the overall aspect of the VCD spectra (see Figure 2).

ii. Region between 1100 and 1350 cm^{-1} (Range B). IR. For compounds **1**−**4** and **6**−**8**, the IR spectrum here is pretty weak, and observed bands reach at most $\varepsilon_{max} \approx 50 \times 10^3$ cm^2/mol. For molecule **5**, $\varepsilon_{max} \approx 75 \times 10^3$ cm^2/mol for three bands. For molecule **10**, there is one highly intense structured band at 1315 cm^{-1} with $\varepsilon = 370 \times 10^3$ cm^2/mol, and for molecule **9** several bands in this region are intense ($\varepsilon_{max} \approx 140 \times 10^3$ cm^2/mol) but weaker than those in the previous region. This region contains contributions from CH-wagging, rocking, and twisting motions with minor participation of CC stretchings.

VCD. The VCD bands in this region for all molecules and especially for **1**−**4**, in absolute value, are as intense as in the previous region. The bands have more or less alternating signs, but the sum of VCD over the region is often positive. This latter fact is similar to what happens in region A, except that in A the sum of rotational strengths is negative. The observed sign alternation of VCD instead makes region B markedly different from region A and is reminiscent of excitonic-type features. We will see below that VCD in region B is generated, in large part, by a set of NMs (CH-wagging, rocking, twisting modes) that contribute exclusively to this region. However, some

TABLE 3: Definition of Group Coordinates for the Construction of the Potential Energy Distribution (PED) and for Defining the Dependence of Rotational Strengths from Single Normal Mode Contributions (See Text)

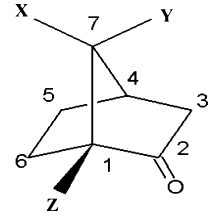

group	coord name[a]	definition
methyl labeled X, Y, and Z	symd, asyd, asyd'	methyl deformation (a)
	rock, rock'	methyl rocking (a)
	tX,tY,tZ	methyl torsions
methylene labeled by C number	sc	scissoring (b)
	rock, wag, twist	(a)
methine	rock, rock'	(a)
CO,(CS)	ip	in-plane bending
	op	out-of-plane bending
C1	rock	2(C7−C1−CZ)−(C2−C1−CZ)−(C6−C1−CZ)
	rock'	(C2−C1−CZ)−(C6−C1−CZ)
C7	sc	XCY scissoring
	rock, wag, twist	(a)
bridge coordinates (b)[b]	sydbrid1,asdbrid1	deformation at C1 (a)
	sydbrid4,asdbrid4	deformation at C1 (a)
	ombrid	bridge CCC
	tbrid1, tbrid4	bridge torsions
six memb. ring coord (b)[b]	trigd	trigonal def. (a)
	asdrin asdrinp asym.	ring def. (a)
	puck	ring puckering (a)
	astrin, astrinp	ring torsions (a)

[a] The first character of the name used in the PED values of Tables 1 and 2 indicates the carbon position in the molecule. [b] As recommended in ref b for norbornane, we used a redundant set of coordinates comprising coordinates of the six-membered ring and treating the bridge as a chain. An alternative choice, using coordinates of the two five-membered rings, was also tried. (a) Pulay, P.; Fogarasi, G.; Pang, F.; Boggs, J. E. *J. Am. Chem. Soc.* **1979**, *101*, 2550−2560. (b) Fogarasi, G.; Zhou, X.; Taylor, P. W.; Pulay, P. *J. Am. Chem. Soc.* **1992**, *114*, 8191−8201.

residual CC-stretchings linger through from the previous region. We observe an almost perfect sign alternation in **1**, while in **2**, **3**, and **4** some change is noticed at ∼1250 cm^{-1}. The couplet observed in **2** corresponding to NMs 40, 41, 42 loses intensity with deuteration and bromination of position 1 in compounds **3** and **4**, respectively. In the latter compound, bromination intensifies the couplet attributed to NMs 37−39. In **5**, all VCD bands of this region are intensified due to the presence of C═S (vide infra). In **6**, the sign alternation is not good, and again for **7**, **8**, and **9** the alternation is almost perfect. Molecule **10** is more evidently an exception due to the group of features above 1300 cm^{-1}. This is due to the presence of the nitramide group and is tied to the large value of the IR intensity of the same group of bands.

iii. Region between 1350 and 1600 cm^{-1} (Range C). IR. For all molecules, one observes five IR features, some of them being broad; in **6**, one has six distinct bands plus a shoulder, and in **8** one has four very congested bands. The bands have similar intensities (with $\varepsilon_{max} \approx 100 \times 10^3$ cm^2/mol) in all of the molecules. The lower frequency group of bands, below 1450 cm^{-1}, is mostly due to NMs containing bending symmetric deformations of CH_3 groups; the higher frequency group, above 1450 cm^{-1}, comes from methylene scissors and antisymmetric deformations of CH_2 groups (vide infra).

VCD. The VCD is generally weak here, reaching $\Delta\varepsilon_{max} \approx 0.01 \times 10^3$ cm^2/mol for all 10 molecules. The first group of bands in the region, below 1450 cm^{-1}, adds up to a negative overall value for the rotational strengths, with the exception of **6** (paralleling the situation of range A), and with some positive contributions for **7**−**10**. The second group of bands, above 1450 cm^{-1}, shows a positive doublet for **1**−**5** and **8**−**10**, while **6** and **7**'s VCD features add up to a negative overall value for the rotational strengths. The sum of the VCD features in the whole region C is close to zero (or slightly positive) in all cases; the conservativeness of the VCD spectra may be attributed to the NMs being generated by vibrations that do not participate in other modes of other spectroscopic regions, i.e. HCH bendings.

Consideration of all of the molecules proposed here suggests a definition of a skeletal chiral sense for camphor. The VCD spectra of molecules **1**−**5** show that the two regions A and C are good indicators for it; compounds **6**, **7**, and **8**, and camphorquinone (not reported here), and the predicted VCD spectrum of epicamphor show the possible extentions and limitations of these diagnostic spectral region. Considering compound **6** and especially (1*S*,4*S*)-epicamphor, we see that their VCD spectra are largely mirror images of camphor's VCD spectrum; however, the different position of the methyl with respect to the carbonyl changes somewhat the vibrational modes and the corresponding bands between 1000 and 1150 cm^{-1}. Region C in camphor and in epicamphor is again a mirror image (the doublet 1455 and 1472 cm^{-1} contains contributions from methylene scissor modes that are substituted by olefinic CH in compound **6**). Compound **7** presents a mixture of signals of camphor and epicamphor. Camphorquinone and compound **8** present (like camphor) a negative VCD below 1100 cm^{-1} and the positive doublet above 1450 cm^{-1}.

In conclusion, we have seen that the three spectroscopic regions (A, B, and C) that we have introduced behave differently regarding, for example, the prevalence of a sign of rotational strengths. The reason may be that they contain bands originated

TABLE 4: Dependence of the Rotational Strengths (10^{-44} esu^2 cm^2) on Group Coordinates for Two Selected Vibrational Modes, Mode 32 (1061 cm^{-1}) and Mode 59 (1821 cm^{-1}) in (1*R*)-Camphor (1)[a]

NM 32 (1061 cm^{-1}; $R = -38.1 \times 10^{-44}$ esu^2 cm^2)				NM 59 (1821 cm^{-1}; $R = 18.0 \times 10^{-44}$ esu^2 cm^2)			
λ	μ	$R^S_{\lambda\mu}$	R_{part}	λ	μ	$R^S_{\lambda\mu}$	R_{part}
ipCO	OpCO	−19.66	−19.66	Asdrin	C2O	−48.18	−48.18
ipCO	6twist	−15.24	−34.91	Asdrin	C2O	34.78	−13.40
C2C3	OpCO	−14.55	−49.45	sydbri	C2O	34.62	21.22
ipCO	3rock	13.86	−35.59	Trigd	C2O	−28.69	−7.47
ipCO	Xrock'	13.23	−22.36	asdbri	C2O	26.84	19.37
ipCO	5rock	12.16	−10.20	1rock'	C2O	−24.78	−5.41
ipCO	Astrin	11.72	1.52	C2C3	C2O	17.07	11.66
ipCO	Astrin	11.18	12.69	1rock	C2O	12.85	24.52
ipCO	Puck	−9.73	2.97	C2O	C2O	−12.26	12.26
asdrin	C2C3	−9.63	−6.67	Asdrin	C2C3	−3.91	8.35
astrin	C2C3	9.50	2.83	C1C2	C2O	3.86	12.22
3rock	C1C2	8.40	11.23	Trigd	C2C3	−3.58	8.63
astrin	C2C3	8.21	19.43	C1C2	C2C3	3.41	12.05
puck	C2C3	−8.13	11.31	sydbri	C2C3	3.19	15.24
ipCO	Yrock'	−7.81	3.49	Zasyd	C2O	−3.18	12.06
6twist	C2C3	−7.75	−4.26	Yasyd'	C2O	3.05	15.11
ipCO	6rock	−7.42	−11.68	TZ	C2O	2.91	18.02
ipCO	asdrin	−6.92	−18.60	3twist	C2O	−2.58	15.44
astrin	C1C2	6.01	−12.59	asdbri	C2C3	2.53	17.96
xrock'	C2C3	5.92	−6.67	tbrid1	C2O	−1.99	15.97
5rock	C2C3	5.84	−0.83	Zrock	C2O	1.89	17.86
ipCO	4rock'	5.67	4.84	Zasyd'	C2O	1.84	19.70
Trigd	C2C3	5.66	10.50	Astrin	C2O	1.83	21.53
C1C2	OpCO	−5.57	4.94	Astrin	C2O	1.66	23.20
ipCO	Trigd	5.03	9.97	3rock	C2O	−1.62	21.58
C1C2	C2C3	−4.75	5.22	6wag	C2O	−1.60	19.97
ipCO	4rock	−4.25	0.97	Zrock'	C2O	−1.59	18.38
6twist	C1C2	−3.99	−3.02	Xrock'	C2O	−1.58	16.80
Yrock'	C2C3	−3.91	−6.93	3wag	C2O	1.56	18.36
6rock	C2C3	−3.72	−10.65	1rock'	C2C3	−1.54	16.82
5rock	OpCO	3.29	−7.35	tbrid4	C2O	−1.40	15.43
Tbrid4	C2C3	−3.20	−10.56	C1C2	C1C2	−1.32	14.11
ipCO	5wag	−3.17	−13.73	Trigd	asdrin	1.32	15.43
sydbri	C2C3	2.97	−10.76	Asdrin	C1C2	−1.27	14.16
puck	C1C2	−2.76	−13.52	Asdrin	C1C2	1.18	15.35
3rock	6rock	2.67	−10.85	5rock	C2O	−1.17	14.17
3rock	6twist	2.66	−8.19	Puck	C2C3	1.15	15.33
4rock'	C2C3	2.66	−5.53	7wag	C2O	1.12	16.45
3rock	4rock'	2.57	−2.96	7twist	C2O	−1.03	15.42
6twist	Astrin	2.51	−0.45	C2O	C4C7	1.02	16.44

[a] Contributions are listed in descending order of absolute value. The first 40 terms are displayed, as discussed in the text. Columns λ and μ contain the group variables as defined in Table 3; $R^S_{\lambda\mu}$ is the corresponding contribution to the rotational strength (see text), and R_{part} is the sum of all of the terms $R^S_{\lambda\mu}$ from the beginning of the list to the current couple of coordinates.

by three different types of NMs, which are generated by valence internal coordinates contributing mostly to one region or the other and whose form does not drastically change from molecule to molecule. The regions A, B, and C may be used independently for diagnostic purposes, and the appearance of their IR and/or VCD spectrum is influenced to a minor extent by the chemical group in position 1 and, to a larger extent, 3 and 2. This, in principle, may be of some help for immediate diagnosis of the absolute configuration of camphor-type molecules, or to monitor whether the substituent groups at one of the carbon atoms in positions 1−7 have altered the normal camphor IR or VCD spectrum.

Roughly speaking, region A contains NMs due mostly to CC stretchings, region B contains NMs due to CH_2-waggings, rockings, twistings plus CC-stretchings, and region C contains NMs due to HCH-bendings only. To prove that the division of the spectra into three regions is not merely empirical, but has its justification in the different types of modes recalled above, we report in Tables 1 and 2 for (1*R*)-camphor (**1**) and (1*R*)-thiocamphor (**5**), respectively, the NM #, the calculated ω (cm^{-1}), the calculated dipole and rotational strengths *D* and *R* (in units of 10^{-40} and 10^{-44} esu^2 cm^2, respectively), and their PED for the vibrational transitions from 900 to 1900 cm^{-1} (see also Table 3). The idea of using the PED in finding correlation patterns in different molecules had been proposed a long time ago by Shimanouchi,[8] but has recently received some attention in VCD studies for the analysis of both rigid and flexible molecules.[9,10] To calculate the PED, we have written our own code, which works in conjunction with Gaussian 03, but we have verified that similar results are obtained when we employ the program MOLVIB(v.7.0), written by Sundius.[20] The definition of PED used in this work is:

$$\mathrm{PED}_{n\lambda} = \frac{L^2_{\lambda n} F_{\lambda\lambda}}{\sum_{\mu} L^2_{\mu n} F_{\mu\mu}} \qquad (1)$$

where *n* is the index of the normal mode under study, λ is the index of the internal coordinate, $L_{\lambda n}$ is the transformation matrix

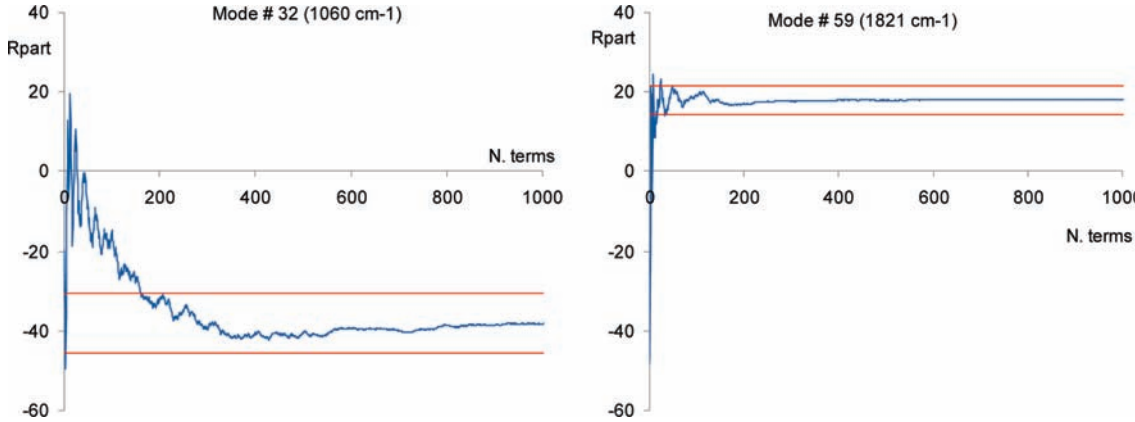

Figure 3. Partial value of the calculated rotational strength in 10^{-44} esu^2 cm^2 as a function of the number of $R^S_{\lambda\mu}$ terms included in the sum of eq 11 in the text, for normal mode number 32 (left) and normal mode number 59 (left) in (1*R*)-camphor (**1**). The contributions in eq 11 are considered in descending order of absolute value.

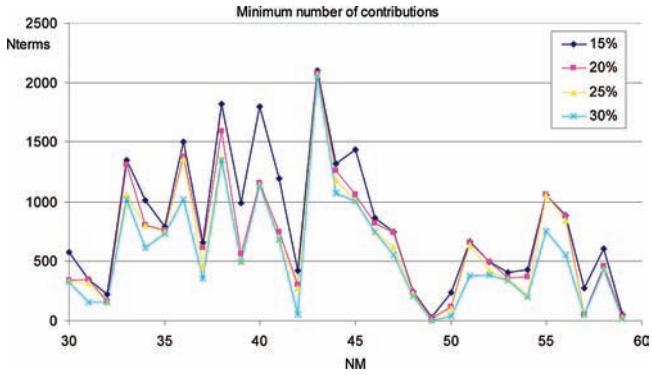

Figure 4. Minimum number of $R^S_{\lambda\mu}$ contributions (given in the *y*-axis) needed in the sum of eq 11 to obtain a value of the rotational strengths reported in the *x*-axis within the 15−30% ranges specified in the figure from the total value for all normal modes from #30 to #59 in (1*R*)-camphor (**1**).

from normal to internal coordinates, $F_{\lambda\mu}$ is the force−constant matrix in internal coordinates, and, because off-diagonal matrix elements are neglected, the PED values are normalized to have their sum equal to 1 (normalization factors range from 0.93 to 1.16 for the vibrations reported in Tables 1 and 2). Cartesian force constants are taken from the Gaussian 03 ab initio calculations. We have employed the definition of internal group coordinates from Pulay et al.,[21] based on Wilson valence coordinates.[22] The group coordinates and the nomenclature employed in the analysis of Tables 1 and 2 are given in Table 3. Looking at Tables 1 and 2, we see that, in accord with what was previously observed, the sum of calculated rotational strengths in region A is negative (−35 for **1** and −77 for **5**), in region B is positive (+40 for **1** and +62 for **5**), and is closer to zero in region C (+6 for **1** and +11 for **5**). In addition, for camphor the most intense mode in region A is calculated at 1061 cm^{-1} in the harmonic approximation; this mode has negative rotational strength and is a mixed NM, containing a high percentage of CC-stretching (adjacent to the carbonyl), plus some C═O in-plane bending. (CC stretchings participate in several NMs in region A.) Region B is largely due to the HCC deformations of CH_2, waggings, rockings, twistings, but contains still some contributions from CC-stretchings. The calculated dipole strengths are smaller than in region A, but the calculated rotational strengths are large and alternate in sign. Region C is due to HCH deformations only, the ones at lower frequency pertaining to the symmetric deformations of the three CH_3 groups X, Y, and Z, and the ones at higher frequency to HCH bendings of CH_2 groups and antisymmetric deformations of CH_3 groups. Table 2 is not too different from Table 1 except that in region B one may trace in the NMs calculated at 1153, 1240, 1309, and 1351 cm^{-1} important contributions from the C═S stretching. This gives high dipole strengths to the NMs, because the C═S bond bears a high dipole moment, in very much the same way as the C═O, whose corresponding NM, though, is calculated to be localized at 1821 cm^{-1}, as in Table 1.

We considered an alternative way for band assignment, not based on PED but on the contribution of each internal coordinate to rotational strengths. In Table 4, we give the dependences on group coordinates of two rotational strengths of (1*R*)-camphor chosen as examples, as done previously in ref 9 for (1*R*)- and (1*S*)-butanol.

The dependence of rotational strengths *R* on internal coordinates is analyzed as suggested in ref 9. The usual expressions of the rotational strength associated with the vibrational transition for normal mode *n* in Cartesian coordinates are:[17]

$$R(n) = \vec{\mu}(n) \cdot \vec{m}(n) \tag{2}$$

$$\mu_i(n) = \sum_{\alpha j} P^{\alpha}_{ij} S_{\alpha j,n} \sqrt{\frac{\hbar}{2\omega_n}} \tag{3}$$

$$m_i(n) = 2\hbar \sum_{\alpha j} A^{\alpha}_{ij} S_{\alpha j,n} \sqrt{\frac{\hbar\omega_n}{2}} \tag{4}$$

where $S_{\alpha j,n}$ is the transformation matrix from Cartesian to normal coordinates, P^{α}_{ij} is the atomic polar tensor (APT), and A^{α}_{ij} is the atomic axial tensor (AAT) for atom α. The corresponding quantities in internal coordinates are derived, by use of the transformation matrix $B_{\lambda,\alpha j}$ from Cartesian to internal coordinates, as

$$P^{\alpha}_{ij} = \sum_{\lambda} \tilde{P}_{i\lambda} B_{\lambda,\alpha j} \tag{5}$$

$$A^{\alpha}_{ij} = \sum_{\lambda} \tilde{A}_{i\lambda} B_{\lambda,\alpha j} \tag{6}$$

$$\mu_i(n) = \sum_{\lambda} \tilde{P}_{i\lambda} L_{\lambda n} \sqrt{\frac{\hbar}{2\omega_n}} \tag{7}$$

$$m_i(n) = 2\hbar \sum_{\lambda} \tilde{A}_{i\lambda} L_{\lambda n} \sqrt{\frac{\hbar\omega_n}{2}} \tag{8}$$

where $L_{\lambda n} = \sum_{\alpha j} B_{\lambda,\alpha j} S_{\alpha j,n}$ is the already mentioned transformation matrix from normal to internal coordinates.

The rotational strength of normal mode n is now written as

$$R(n) = \hbar^2 \sum_{\lambda\mu} \sum_{i} \tilde{P}_{i\lambda} L_{\lambda n} \tilde{A}_{i\mu} L_{\mu n} = \sum_{\lambda\mu} R_{\lambda\mu}(n) \tag{9}$$

Symmetrized expressions are then considered for the contributions appearing in the last sum:

$$R^{S}_{\lambda\mu}(n) = R_{\lambda\mu}(n) + R_{\mu\lambda}(n) - \delta_{\lambda\mu} R_{\lambda\mu}(n) \tag{10}$$

so that the total rotational strength is now obtained as

$$R(n) = \sum_{\lambda \geq \mu} R^{S}_{\lambda\mu}(n) \tag{11}$$

Considering just a few large terms in the previous sum as responsible for the rotational strength under study would be desirable. Yet because n_i is the number of internal coordinates involved in our calculations, the number of terms, $n_i(n_i + 1)/2$, contributing to the sum in eq 11 is about 3000, so it is not easy to isolate the really significant ones, keeping also in mind that they may alternate in sign. In particular, we studied normal modes from 30 to 60, corresponding to the frequency region of Figure 1: if the terms in the sum of eq 11 are organized in descending order of absolute value, and one wants to truncate the sum at a point from which the result permanently lies in a range of 20% around the correct value (given by the complete sum), a very large number of terms is in general needed. As an example, a list of the first 40 contributions for two selected normal modes is reported in Table 4, where each row contains not only $R_{\mu\lambda}{}^{S}$ but also the partial value R_{part} of the rotational strength, the latter quantity being obtained as the sum of the contributions for all couples of coordinates up to the one under examination. The quantity R_{part} is plotted in Figure 3 for the two selected normal modes, number 32 at 1061 cm^{-1} and number 59 at 1821 cm^{-1}, as a function of the number of contributions (always in descending order of absolute values); moreover, two horizontal lines are shown in each plot at ±20% from the final value of the rotational strength (which is the rightmost plotted value). For normal mode number 32, to have R_{part} within 20% of the total rotational strength, one has to consider at least 160 terms, and this number does not significantly decrease if the range is extended to ±30%. A more useful situation occurs for mode number 59, where 37 terms are enough to reach a stability within 20%, and just 16 are needed for reproduction of the final value within 30% accuracy. The latter

TABLE 5: Calculated Frequencies (ω, cm^{-1}), Rotational Strengths (R, 10^{-44} esu^2 cm^2), Robustness Angle (φ, deg), and Robustness Evaluation (ev) in the Mid-IR Region for the First Five Compounds Shown in Scheme *I* (in the Interval 900−1850 cm^{-1})[a]

1 (camphor)					**2**					**3**					**4** (bromocamphor)					**5** (thiocamphor)				
NM	ω	R	φ	ev	NM	ω	R	φ	ev	NM	ω	R	φ	ev	NM	ω	R	φ	ev	NM	ω	R	φ	ev
24	925.65	−12.10	124	r	21	932.8	−30.20	145	r*	21	899	−11.90	124	r	23	934.2	59.60	47.4	r	24	921.28	−48.20	156	r*
25	939.89	26.30	50.9	r	22	944.5	22.50	65.2	r	22	922.9	13.30	70	r	24	944.8	−87.30	158	r*	25	933.56	29.50	14.1	r*
26	951.19	12.80	40.1	r*	23	953.6	−7.91	105	r	23	946.1	−12.00	136	r*	25	959.5	21.00	40.7	r*	26	953.97	6.55	73.8	r
27	956.81	−2.77	96.7	w	24	960.8	5.33	57.9	r	24	959	−0.74	102	w	26	963.9	1.50	88.7	w	27	958.85	−4.71	112	r
28	966.84	−11.20	128	r	25	976.8	−2.62	95.7	w	25	959.8	7.85	69	r	27	980.1	−1.99	92.9	w	28	962.85	0.03	90	w
29	1003.5	−3.61	112	r	26	1009	−6.18	165	r*	26	994.8	18.80	42	r*	28	1001	−17.40	115	r	29	1002.1	−5.70	124	r
30	1029.7	7.64	42	r*	27	1030	−13.50	109	r	27	1003	−1.89	107	r	29	1023	−31.80	144	r*	30	1021.2	−11.30	116	r
31	1038.9	−15.50	98.9	w	28	1053	23.80	68.7	r	28	1027	−23.30	128	r	30	1051	5.56	70.9	r	31	1032	−28.70	153	r*
32	1059.6	−38.00	114	r	29	1087	−27.50	121	r	29	1066	−17.20	137	r*	31	1078	11.70	80.1	w	32	1047.5	−8.14	142	r*
33	1097.3	1.80	87.1	w	30	1130	−18.50	110	r	30	1086	6.71	76	w	32	1092	−20.10	170	r*	33	1097.5	−6.11	103	w
34	1113.7	−5.78	95.1	w	31	1146	−3.08	104	w	31	1101	−31.00	109	r	33	1133	1.49	81.7	w	34	1110.9	−23.70	115	r
35	1147.7	8.91	60.7	r	32	1170	−0.87	96.7	w	32	1132	−10.10	121	r	34	1159	2.66	79.5	w	35	1139.4	26.80	40.4	r*
36	1172.2	−6.40	150	r*	33	1198	14.00	43.2	r*	33	1159	−0.81	94	w	35	1199	9.91	23.3	r*	36	1151.5	−62.40	139	r*
37	1189.3	19.70	43.9	r*	34	1215	−1.06	95.1	w	34	1203	7.99	47	r	36	1224	0.40	89.4	w	37	1184.5	51.90	22.6	r*
38	1215.9	−2.49	107	r	35	1242	−1.71	93.2	w	35	1222	−0.81	93	w	37	1237	−11.60	116	r	38	1200.1	3.45	84.3	w
39	1223.1	−5.06	106	r	36	1245	−10.60	109	r	36	1241	−2.20	93	w	38	1261	13.90	45.8	r	39	1219.3	−11.70	104	w
40	1247.2	2.07	84.6	w	37	1263	8.51	20.6	r*	37	1259	−0.64	93	w	39	1267	35.90	35.9	r*	40	1238.9	26.20	53.1	r
41	1266.5	2.85	43.9	r*	38	1272	10.30	32.4	r*	38	1269	23.70	36	r*	40	1282	−0.36	90.3	w	41	1245.9	−35.90	150	r*
42	1274.1	26.10	27.3	r*	39	1293	17.80	77.9	w	39	1283	11.30	81	w	41	1319	−4.49	106	r	42	1269.3	13.40	49	r
43	1302.2	−1.08	93.2	w	40	1323	−6.31	153	r*	40	1318	−3.36	115	r	42	1324	2.46	85.9	w	43	1295.2	19.90	62.3	r
44	1325.7	−7.07	108	r	41	1328	−8.55	132	r	41	1325	1.84	86	w	43	1331	3.02	81.7	w	44	1308.1	48.90	14.5	r*
45	1331.1	−3.42	101	w	42	1344	17.80	14.8	r*	42	1329	6.11	70	r	44	1402	−2.76	109	r	45	1323.8	−4.41	97.3	w
46	1350.5	9.25	67.4	r	43	1402	−2.00	113	r	43	1402	−1.77	112	r	45	1421	−5.40	154	r*	46	1338.5	17.30	72.8	r
47	1398.9	−0.97	105	r	44	1421	−5.47	162	r*	44	1420	−5.19	166	r*	46	1452	−5.75	125	r	47	1349.7	−3.50	93.2	w
48	1405.2	3.82	51.2	r	45	1454	−3.92	127	r	45	1454	−4.07	122	r	47	1477	−1.88	146	r*	48	1400.7	−3.66	128	r
49	1419.9	−9.02	159	r*	46	1480	−1.72	107	r	46	1480	−1.72	107	r	48	1487	−1.36	93.8	w	49	1408.5	0.17	88.7	w
50	1451.4	−5.06	119	r	47	1487	−1.36	97.3	w	47	1487	−1.43	98	w	49	1494	0.91	78.9	w	50	1421.4	−5.74	141	r*
51	1478	−1.72	106	r	48	1495	3.53	72.2	r	48	1495	3.40	72	r	50	1506	3.55	0	r*	51	1451.9	−1.54	97.3	w
52	1481.3	−2.17	102	w	49	1507	−0.20	97.9	w	49	1506	0.08	87	w	51	1513	12.50	67.1	r	52	1476.2	−0.06	90.3	w
53	1486.3	7.39	22.6	r*	50	1513	8.70	63.6	r	50	1512	8.46	64	r	52	1522	−5.31	130	r	53	1480.6	1.94	82.4	w
54	1493.2	3.58	78.5	w	51	1520	−4.27	132	r	51	1520	−3.95	128	r	53	1844	35.50	84.3	w	54	1486.4	8.76	38.5	r*
55	1497.4	−0.50	92.2	w	52	1825	11.30	85.2	w	52	1823	14.50	84	w						55	1490.4	0.74	88.1	w
56	1509.2	1.38	37.5	r*																56	1499.6	−3.01	111	r
57	1513.2	14.00	49.9	r																57	1507.3	0.37	77.9	w
58	1527.9	−1.54	109	r																58	1511.7	19.70	51.2	r
59	1819.6	17.90	85.9	w																59	1519.7	−10.20	157	r*

[a] Normal modes are defined weak (w) if φ is within 15° from a right angle, and robust (r*) if it falls outside the range (90° − 45°, 90° + 45°); the rest of the modes are classed as intermediate (r).

TABLE 6: Calculated Overlap Parameter (Ω) for Selected Normal Modes of Compounds 1 and 2 of Scheme 1 (See Text)[a]

1 (camphor)			**2**			
NM	ω	R	NM	ω	R	Ω
59	1819.6	17.9	52	1824.6	11.3	0.999
57	1513.2	14.0	50	1512.6	8.7	0.988
50	1451.4	−5.1	45	1454.2	−3.9	−0.998
50	1451.4	−5.1	44	1420.7	−5.5	−0.029
46	1350.5	9.3	42	1343.6	17.8	−0.667
42	1274.1	26.1	38	1272.1	10.3	−0.885
37	1189.3	19.7	33	1197.6	14.0	0.332
32	1059.6	−38.0	29	1087.3	−27.5	0.551
31	1038.9	−15.5	27	1030.1	−13.5	−0.266
29	1003.5	−3.6	26	1009.2	−6.2	0.892

[a] NM, mode number; ω, frequency (cm^{-1}); R, rotational strength (10^{-44} esu^2 cm^2).

normal mode can be meaningfully analyzed using Table 4, where the dominant role of variable C2O, corresponding to CO stretching, is apparent. This analysis limits the universal applicability of an assignment method of the IR and VCD bands, based on the partitioning of the calculated rotational strengths in terms of local internal group coordinates. For a bird's eye view of possibly defining the transitions associated with the normal modes in the mid-IR region for compound **1**, we plot in Figure 4 the number of terms needed for approximations within 15%, 20%, etc., as functions of NM#. Of course, the attribution of a VCD band associated with a normal mode to a given internal coordinate or to a small number thereof is sensible if this number is small; this appears to happen for very few normal modes. From the above discussion, also the assignment based on the analysis of PED poses some problems. In any case, we think a quantitative analysis (PED or $R_{\mu\lambda}^{S}$) is safer than the mere inspection of the normal modes, as in, for example, GAUSSVIEW. Recently, an analysis of the "stability" of rotational strengths of given normal mode (NM) transitions with respect to perturbations due to substitutions of groups was proposed by Nicu et al.[11] The cited authors propose as a discriminating parameter the angle φ formed by the electric and magnetic dipole transition moments $\vec{\mu}(n)$ and $\vec{m}(n)$ of eqs 3 and 4, respectively. We performed such calculations and provide the results for molecules **1**−**5** in Table 5, where we indicate NMs according to their "robustness" in the spirit of what was proposed in ref 11. We also indicate in Figure 1 the most robust NMs indicated as r* in Table 5 (please notice that the same NM numbering is used in Figure 1 and in Table 5); finally, we give in the Supporting Information a figure, where we superimpose the φ-parameter to the calculated VCD spectrum for molecule **1**. One may notice that quite a few prominent calculated (and observed) VCD features are due to r*-"robust" modes. There are few exceptions to that, and we wish to point out the behavior of an important VCD feature, most used in conformational analysis, associated with the carbonyl stretching mode:[23] the latter mode is indeed calculated as not being robust. On this basis, we carried out some further analysis, also suggested, in ref 11: we calculated the degree of dynamical overlap of NM in molecules **1** and **2** for NM pairs carrying similar rotational strengths and similar φ. The results are given in Table 6. The overlap parameter Ω is defined as follows for a selected (n,m) pair of NMs in molecule **1** and **2**, respectively:

$$\Omega_{nm} = \frac{\sum_{\alpha j}^{*} S_{aj,n}(1) S_{\alpha j,m}(2)}{\sqrt{\left(\sum_{\alpha j}^{*} |S_{\alpha j,n}(1)|^2\right) \cdot \left(\sum_{\alpha j}^{*} |S_{\alpha j,m}(2)|^2\right)}} \qquad (12)$$

In eq 12, a star reminds the reader that the sums are limited to atoms that are common to the two considered molecules. The $S_{\alpha j,n}$ transformation matrix coefficients from NMs to atomic Cartesian coordinates were defined above and are employed here. Of course, they are calculated in a common right-handed Cartesian coordinate system, where the z axis coincides with the C═O bond and the y axis lies in the OC_2C_1 plane (see Scheme 1). As one may see from Table 6, the carbonyl stretching mode (NM #59 and 52 in the two molecules) exhibits the highest overlap factor Ω, whereas in other cases, for example, the (32,29) pair, the correlation is small. We would like also to remind that recently Hug et al.[24] have discussed a "similarity parameter" for ROA and VCD spectra that bears some resemblance to the overlap parameter defined in ref 23 and recalled in eq 12.

In conclusion, we suggest that all four criteria presented here are worthwhile to consider, because they all help to discover common, and sometimes independent, characteristics of the studied VCD spectral features.

b. Behavior of Flexible Groups in Positions 3 (Molecules* 8 *and* 9 *of Scheme 1) and 2 (Molecule* 10 *of Scheme 1). In principle, these three molecules contain mobile groups. How-

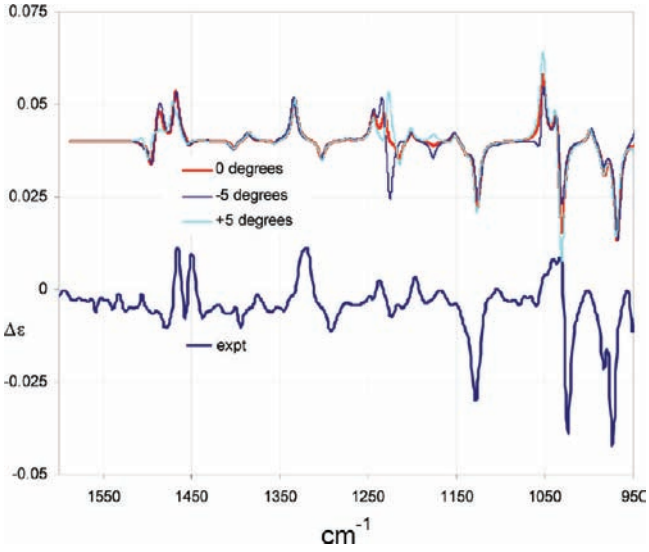

Figure 5. Comparison of experimental (bottom) and calculated (top) (B3PW91/TZ2P) VCD spectra for the minimum energy conformation and two other conformations for τ(OCCO) = ±5° for compound **9** (see text).

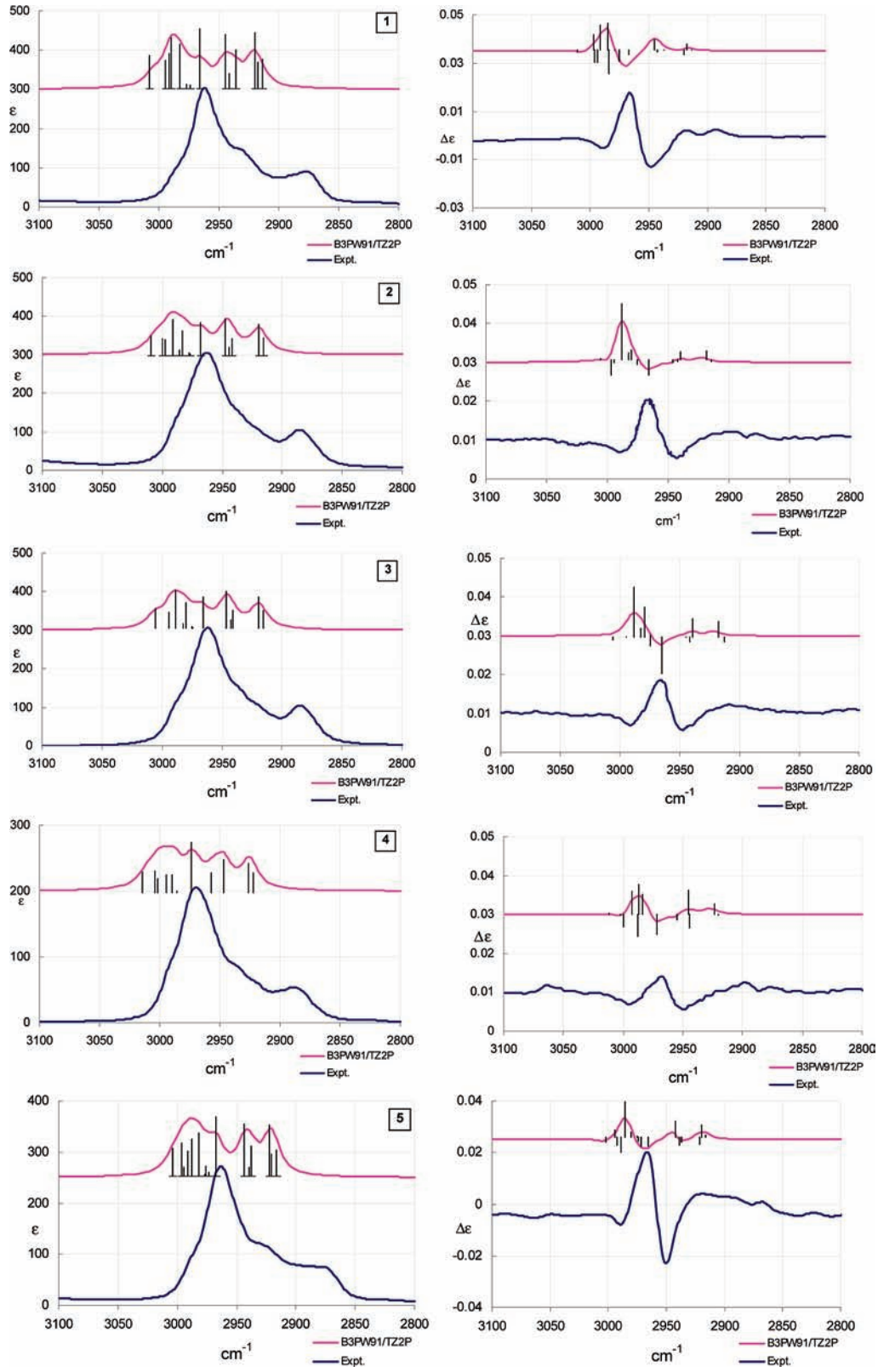

Figure 6. Experimental and calculated IR absorption (left) and VCD (right) spectra in the CH-stretching region for molecules **1**−**5** in Scheme 1. In all graphs, ε and $\Delta\varepsilon$ are in 10^3 m^2 mol^{-1} units (VCD experimental data for **1** and **5** taken in Brescia; **2**, **3**, and **4** taken at the University of Minnesota).

ever, from the analysis of calculated relative energy and free energy values, we checked that molecules **8** and **10** possess one predominant conformation. We think that in both cases this is related to the *E*-configuration of the double C═N bond. In contrast, in molecule **9**, the five-membered ring in position 2 is quite conformationally mobile. Indeed, if one calculates the conformational energy versus the dihedral angle OCCO, one obtains a fairly flat curve. With a B3LYP/6-31G** basis, we obtain a curve with a minimun close to OCCO = 0° and increasing by 0.15 kcal/mol in the range ±30°. This indicates that there is a large amplitude puckering motion for the five-membered ring. As was previously done,[13,14] in Figure 5 we

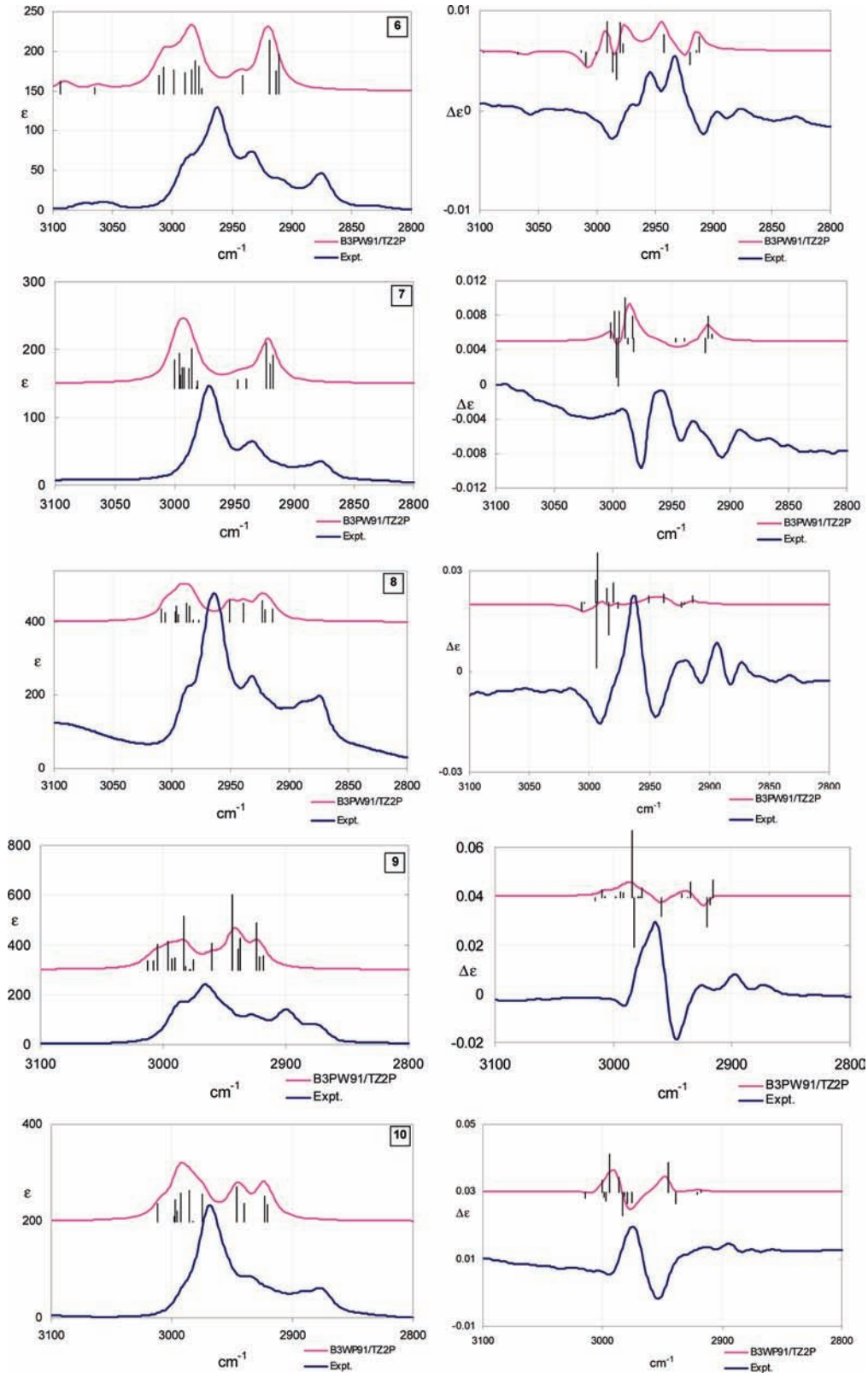

Figure 7. Experimental and calculated IR absorption (left) and VCD (right) spectra in the CH-stretching region for molecules **6**−**10** in Scheme 1. In all graphs, ε and $\Delta\varepsilon$ are in 10^3 cm^2 mol^{-1} units.

compare the experimental VCD spectra with the superimposed calculated VCD spectra for dihedral angle τ(OCCO) = 0°, ±5° (the spectra calculations were conducted at B3PW91/TZ2P level). One may see that the largest VCD differences for the three situations are observed at ca. 1200 cm^{-1}, where the five-membered ring has VCD features associated with fairly localized and defined NMs. The sum of the two spectra corresponding to τ(OCCO) = ±5° presents two negative features in correspondence with experimental ones at 1215, 1226 cm^{-1}, indicating that the distorted geometries are possible. In the other regions of the VCD spectrum, the three pseudoconformers give quite similar features. The IR spectra for the three situations are the same in all regions (in Figure 2 were given the results for the calculated IR and VCD spectra for τ(OCCO) = 0°).

c. The CH-Stretching Region (2800−3200 cm^{-1}). Also for this region, constant motifs may be found in the VCD spectra and have been evidenced and commented previously.[7,15,25] Because the largest VCD features that were commented in ref 7 were found to be independent of the chemical function of position 2, they were identified as due to geometrical factors, that is, the relative orientation of CH_2, CH, and CH_3 groups, depending on the skeletal chiral sense introduced and discussed above, and were attributed to "vibrational excitons", as of the definition of refs 15 and 25. Here, we wish to discuss additional examples, and we will try to find a rationale for the existence of such "vibrational excitons", based on DFT calculations and on the comparison of the results for camphor-type and norcamphor-type molecules.

The IR spectra of camphor-type molecules consist of a strong and structured band at ca. 2960 cm^{-1} and a broad weaker continuum between 2940 and 2850 cm^{-1}. The broadening of the latter region is due to Fermi resonance (FR), which makes the usability of the corresponding VCD features questionable. Recently,[26] some quantitative evaluations of this phenomenon have been tried with some success, but we will not dwell on that aspect for these molecules: we only observe that also in this part of the spectrum the VCD data show a trend, the sum of VCD being weak and positive for the (1*R*)-configuration of the majority of camphor-type molecules. However, a more evident quite constant VCD motif is found in correspondence of the 2960 cm^{-1} IR absorption feature: a triplet of VCD bands with alternating signs; for the (1*R*)-configuration a (−,+,−) triplet at 2980 cm^{-1} (weak negative VCD), 2960 cm^{-1} (strong positive VCD), 2950 cm^{-1} (strong negative VCD) is observed. In addition to the eight molecules **1**−**5**, and **8**−**10** within the set of molecules **1**−**10** of the present work, this triplet has clearly been observed also for (1*R*)-2-methylene-camphor,[7] and, less clearly but still convincingly, for (1*R*)-camphorquinone, (1*R*)-borneol,[27] and 1-*d*-(1*R*)-camphorquinone.[28] We report in Figures 6 and 7 the comparison of calculated and experimental IR and VCD spectra for camphor-type molecules **1**−**5** and **6**−**10**, respectively (underneath calculated bands we also give bars proportional to calculated dipole and rotational strengths corresponding to calculated frequencies). The triplet is reproduced by the calculations, even though we cannot state that individual calculated features correspond to observed ones. Rather, the algebraic sum of calculated features reproduces experiments. In Figure 8, we juxtapose all of the experimental VCD spectra for an empirical correlation. The correlation is pretty strong, and the (−,+,−) triplet is found everywhere, except in **6** and **7**. This empirical pattern is nicely matched by what happens in fenchone-type molecules, which, for the same (1*R*)-configuration, exhibit the opposite VCD pattern (+,−,+) at similar frequencies, as recognized for four molecules: (1*R*)-fenchone and (1*R*)-2-methylene-fenchone,[7] (1*R*)-thiofenchone,[28] and, to a lesser extent, (1*R*)-fenchyl alcohol.[27] The reason of the common pattern identified throughout camphor and fenchone molecules is the presence of a CH_3 group, especially geminated ones. We base these conclusions on two observations:

(a) When we do not have a nor-CH_3 group like in norcamphor, or 3-aza-norcamphor, or in 7-cyclopropyl-norcamphor, the observed VCD spectrum is very weak (unpublished data from V. M. Pultz et al.[28]).

(b) We further corroborate this point of view by analyzing the assignment of the calculated VCD features reported in Figures 6 and 7, as well as the results for norcamphor-type molecules. In Table 7, we summarize the results for (1*R*)-camphor and (1*R*)-norcamphor cases (to compare with experiment, one should subtract anharmonicity that in this case is about 2χ = 140 cm^{-1}[17,29]). Summing over calculated rotational strengths is necessary, due to the congestion of calculated features observed in Figures 6 and 7, which makes rationalization of the observed features very difficult at first sight. Another aspect hampering the understanding of the apparently simple experimental VCD spectra is also the use of bandshapes in the reproduction of the data; we must admit that well-defined knowledge of the reason for choosing a given bandwidth does not exist yet. We attribute to this a general underestimate of VCD spectra.

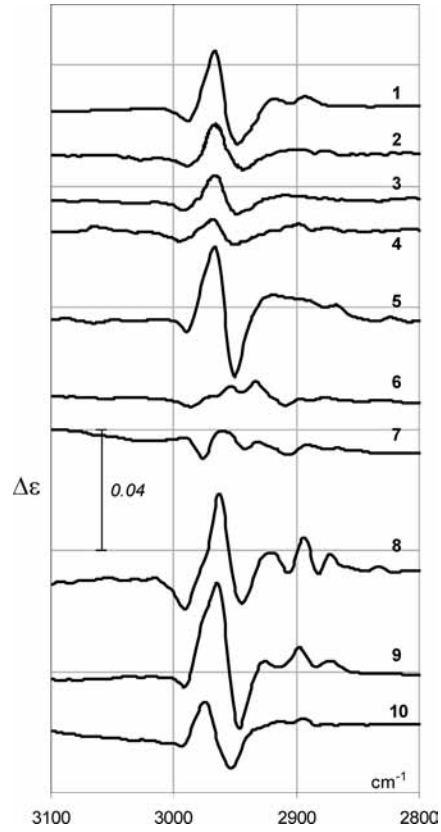

Figure 8. Comparison of the experimental VCD spectra in the CH-stretching region for molecules **1**−**10** of Scheme 1 (VCD experimental data for **1**, **5**, **6**−**10** taken in Brescia; **2**, **3**, and **4** taken at the University of Minnesota).

These findings were derived for B3PW91/TZ2P, but they are independent of the basis set and functional employed in the calculations and have been indeed already presented in ref 7, where B3LYP/6-31G** and B3PW91/TZVP were chosen. As was found for the mid-IR region, we think that the sum of rotational strengths in the CH-stretching regions corresponding to the (−,+,−) triplet is not accidental, but is related to the "skeletal chiral sense" of the molecule. Also, the same conclusions hold for (1*R*)-thiocamphor and other molecules examined here.

The major fact is that when the CH_3 group is present in position 7 for camphor compounds, the feature at ∼3127−3124 cm^{-1} becomes negative, and the next two lower frequency features increase their absolute values. Why geminated CH_3 are so effective in making VCD easier to observe is not fully clear. However, by considering the above scheme, we propose that: (i) they give a negative contribution of their own to the features at ca. 3130 and 3100 cm^{-1}; and (ii) the NM of CH_2 groups are delocalized over too many centers in norcamphor; the presence of CH_3 in camphor interrupts such delocalization, thereby

TABLE 7: Assignment of VCD Calculated Bands[a]

(1*R*)-camphor				(1*R*)-norcamphor			
no. of NMs	assign.	freq. range (cm^{-1})	sum of rot. str. (10^{-44} esu^2 cm^2)	no. of NMs	assign.	freq. range (cm^{-1})	sum of rot. str. (10^{-44} esu^2 cm^2)
1	CH_3	3140	−3	1	1	3145	∼0
3	CH_3(7,1)	3127−3124	−10	1	5,6	3126	+11
3	5,6,3	3122−3115	+32	3	7,3,5,6,4	3116−3115	+14
3	5,6,4,CH_3	3109−3098	−20	1	3,6,4,3	3109	−12

[a] The number of normal modes contributing to each band is given in the first column.

promoting vibrational excitons over limited molecular portions: in particular, the (+,−) intense couplet is associated with contributions of CH-antisymmetric stretchings of positions (5,6) in interactions with CH-local stretchings in positions 3 and 4, respectively.

4. Conclusions

In this work, we have made an effort to identify common VCD features to the mid-IR and CH-stretching VCD spectra of several camphor-type molecules, to make the various regions of the VCD spectra immediately recognizable and separately usable to the general organic chemistry scientists. The minimal or sometimes nonexisting set of conformers has allowed us to obtain a good to excellent prediction of VCD spectra from DFT calculations and then to justify empirical rules derived from experimental data. The mid-IR region (950−1600 cm^{-1}) was partitioned in three ranges A, B, and C containing contributions from different group-frequency NM,[8,21] and in the CH-stretching region the successions of VCD bands of constant signs (−,+,−) for (1*R*)-configurations of all camphor-type molecules were observed and interpreted in terms of vibrational excitons. In the former case, the evaluation of the PED, the partitioning of rotational strengths in internal coordinates' contributions, the study of the angle φ defining the robustness of NMs, and the overlap Ω of NMs in two related molecules have provided some theoretical ground to our findings. The idea of partitioning IR spectra is related to the idea of internal group coordinates and was discussed by Herzberg[29] and Shimanouchi.[8] Furthermore, in the case of VCD, we consider the following sum rule. By carrying through the summation in eq 9 over NMs labeled by n, one has:

$$\sum_n R(n) = \hbar^2 \sum_{\lambda\mu} \left(\sum_i \tilde{P}_{i\lambda} \tilde{A}_{i\mu} \right) \left(\sum_n L_{\lambda n} L_{\mu n} \right) = \hbar^2 \sum_{\lambda\mu} \left(\sum_i \tilde{P}_{i\lambda} \tilde{A}_{i\mu} \right) G_{\lambda\mu} \quad (13)$$

The latter term has been obtained by taking into account that NM eigenvectors written in terms of internal coordinates are normalized to the Wilson G-matrix.[22] An equation similar to eq 13 was derived by Polavarapu,[30a] and commented on further later;[30b] the two approaches may be easily shown to be equivalent, by following Appendix VIII of ref 22. In the present form, it allows one to state that the grand sum of rotational strengths over the entire IR range depends only on charge distribution, through $P_{i\lambda}$ and $A_{i\mu}$, and on masses and geometry, through $G_{\lambda\mu}$. Besides, if there is a partitioning of the G matrix in correspondence of given groups of coordinates, as, for example, in Appendix IX of ref 22 (see Table 3), the grand sum splits into subsums that refer to separate internal coordinate regions.

On this basis, for the mid-IR region, we propose to consider VCD spectra not line-by-line, but rather region-by-region, the sum of the rotational strengths of the bands in two of the regions correlating in sign with what we have defined above as the "skeletal chiral sense" of the molecule. From the PED analysis, we infer that this behavior originates from the differences of the CC-bonds in the vicinity of the asymmetric carbon atom under study. We expect that these rules remain useful in more complex cases than camphors, where the existence of multiple conformations may make the ab initio calculation hard to perform.

The dependence of the sign of the sum of observed rotational strengths over regions A (950−1100 cm^{-1}) (−) and B (1100−1350 cm^{-1}) (+) in the mid-IR region on the "skeletal chiral sense" of (1*R*)-camphor molecules and the correlation with the (−,+,−) succession of signs for the VCD bands in the CH-stretching region between 2980 and 2940 cm^{-1} is expected to work also with other bridged molecules. Indeed, in fenchone-type molecule with the same absolute configuration designation for stereogenic carbons 1 (1*R*) and 4 (4*R*), both the mid-IR regions A and B[7] and the triplet of bands in the CH-stretching region invert in sign, and thus the "skeletal chiral sense" is opposite to that of camphor.

Acknowledgment. We thank MIUR (PRIN2006) for financial support and the "Consorzio Interuniversitario Lombardo per l'Elaborazione Automatica" (CILEA) via R. Sanzio, 4 20090 Segrate (Mi), for kind use of computational facilities. We thank Prof. Sundius, University of Helsinki, Finland, for kindly providing free use of his MOLVIB program. We are grateful to one of the reviewers for useful suggestions.

Supporting Information Available: Comparison of calculated VCD spectra of (1*R*,4*R*)-epicamphor with calculated and experimental VCD spectra of (1*R*,4*R*)-oxocamphor (mid-IR range). Comparison of calculated VCD spectra of (1*S*,4*S*)-epicamphor with calculated and experimental VCD spectra of (1*R*,4*R*)-camphor (mid-IR range). Comparison of experimental and calculated VCD spectra of (1*R*,4*R*)-camphor (mid-IR range): for each normal mode, the robustness parameter φ is superimposed to the calculated spectrum. This material is available free of charge via the Internet at http://pubs.acs.org.

References and Notes

(1) Lightner, D. A.; Gurst, J. *Organic Conformational Analysis and Stereochemistry from Circular Dichroism Spectroscopy*; Wiley−VCH: New York, 2000.

(2) Bouman, T.; Hansen, A. *Adv. Chem. Phys.* **1980**, *44*, 454.

(3) McCann, D. M.; Stephens, P. J. *J. Org. Chem.* **2006**, *71*, 6074–6098.

(4) Devlin, F. J.; Stephens, P. J. *J. Am. Chem. Soc.* **1994**, *116*, 5003–5004.

(5) Nafie, L. A.; Freedman, T. B. In *Circular Dichroism, Principles and Applications*; Berova, N., Nakanishi, K., Woody, R. A., Eds.; Wiley−VCH: New York, 2000; Chapter 4, pp 92−132.

(6) Polavarapu, P. L. *Vibrational Spectra and Structure*; Elsevier: Amsterdam, 1989; Vol. 17B, pp 319−342.

(7) Longhi, G.; Abbate, S.; Gangemi, R.; Giorgio, E.; Rosini, C. *J. Phys. Chem. A* **2006**, *110*, 4958–4968.

(8) Shimanouchi, T.; Nakagawa, I. *Annu. Rev. Phys. Chem.* **1972**, *23*, 217–238.

(9) Shin, S.; Nakata, M.; Harmada, Y. *J. Phys. Chem. A* **2006**, *110*, 2122–2129.

(10) Tanaka, T.; Oelgemöller, M.; Fukui, K.; Aoki, F.; Mori, T.; Ohno, T.; Inoue, Y. *Chirality* **2007**, *19*, 415–427.

(11) Nicu, V. P.; Neugebauer, J.; Baerends, E. J. *J. Phys. Chem. A* **2008**, *112*, 6978–6991.

(12) Devlin, F. J.; Stephens, P. J.; Besse, P. *J. Org. Chem.* **2005**, *70*, 2980–2993.

(13) Setnicka, V.; Urbanovà, M.; Bouř, P.; Kràl, V.; Volka, K. *J. Phys. Chem. A* **2001**, *105*, 9931–8938.

(14) Abbate, S.; Burgi, L. F.; Castiglioni, E.; Lebon, F.; Longhi, F.; Longhi, G.; Toscano, E.; Caccamese, S. *Chirality* **2009**, *21*, 436–441.

(15) Gangemi, R.; Longhi, G.; Lebon, F.; Laux, L.; Abbate, S. *Monatsh. Chem.-Chem. Monthly* **2005**, *136*, 325–346.

(16) **1**: Aldrich. **2**: Lightner, D. A.; Beavers, W. A. *J. Am. Chem. Soc.* **1971**, *267*, 7–2684. **3**: Lightner, D. A.; Crist, B. V.; Flores, M. F. *J. Chem. Soc., Chem. Commun.* **1980**, *27*, 3–275, and refs therein. **4**: Fong, W.; Thomas, R.; Scherer, K., Jr. *Tetrahedron* **1971**, *12*, 3789–3970. **5**: Aldrich; see also: Wijekoon, W. M. D.; Bunnenberg, E.; Records, R.; Lightner, D. A. *J. Phys. Chem.* **1983**, *87*, 3034–3037. **6**: Hutrchinson, J. H.; Kuo, D. L.; Money, T.; Yokoyama, B. *J. Chem. Soc., Chem. Commun.* **1988**, *128*, 1–1282. **7**: Heinane, E. *Suomen Kemistilehti* **1969**, *42*, 53–60. **8**: Aldrich; see also: Cullen, D. L.; Manion, M. M.; Crist, B. V.; Lightner, D. A. *Tetrahedron* **1983**, *39*, 733–742. Roy, S.; Chakraborty, K. *Tetrahedron Lett.* **1988**, *39*, 6335–6336. **9**: Baker, K. M.; Davis, B. R. *Tetrahedron* **1968**, *24*, 1655–1662. **10**: Synthesized and characterized in D. A. Lightner's lab. **11**: Evans, C.; McCague, R.; Roberts, S. M.; Sutherland, A. G. *J. Chem. Soc., Perkin Trans.* **1991**, *1*, 656–657. **12**: Berson, J. A.; Walia, J. S.; Remanick, A.; Suzuki, S.; Warnhoff, P. R.; Willner, D. *J. Am. Chem. Soc.* **1961**, *83*, 3986–3997. **13**: Lightner, D. A.; Beavers, W. A. *J. Am. Chem. Soc.* **1971**, *267*, 7–2684.

(17) Stephens, P. J. *J. Phys. Chem.* **1985**, *89*, 748–751. Stephens, P. J.; Lowe, M. A. *Annu. Rev. Phys. Chem.* **1985**, *36*, 213. Stephens, P. J.; Devlin, F. J.; Chabalowski, C. F.; Frisch, M. J. *J. Phys. Chem. A* **1994**, *98*, 11623.

(18) Frisch, M. J.; Trucks, G. W.; Schlegel, H. B.; Scuseria, G. E.; Robb, M. A.; Cheeseman, J. R.; Montgomery, J. A., Jr.; Vreven, T.; Kudin, K. N.; Burant, J. C.; Millam, J. M.; Iyengar, S. S.; Tomasi, J.; Barone, V.; Mennucci, B.; Cossi, M.; Scalmani, G.; Rega, N.; Petersson, G. A.; Nakatsuji, H.; Hada, M.; Ehara, M.; Toyota, K.; Fukuda, R.; Hasegawa, J.; Ishida, M.; Nakajima, T.; Honda, Y.; Kitao, O.; Nakai, H.; Klene, M.; Li, X.; Knox, J. E.; Hratchian, H. P.; Cross, J. B.; Adamo, C.; Jaramillo, J.; Gomperts, R.; Stratmann, R. E.; Yazyev, O.; Austin, A. J.; Cammi, R.; Pomelli, C.; Ochterski, J. W.; Ayala, P. Y.; Morokuma, K.; Voth, G. A.; Salvador, P.; Dannenberg, J. J.; Zakrzewski, V. G.; Dapprich, S.; Daniels, A. D.; Strain, M. C.; Farkas, O.; Malick, D. K.; Rabuck, A. D.; Raghavachari, K.; Foresman, J. B.; Ortiz, J. V.; Cui, Q.; Baboul, A. G.; Clifford, S.; Cioslowski, J.; Stefanov, B. B.; Liu, G.; Liashenko, A.; Piskorz, P.; Komaromi, I.; Martin, R. L.; Fox, D. J.; Keith, T.; Al-Laham, M. A.; Peng, C. Y.; Nanayakkara, A.; Challacombe, M.; Gill, P. M. W.; Johnson, B.; Chen, W.; Wong, M. W.; Gonzalez, C.; Pople, J. A. *Gaussian 03*, revision B.05; Gaussian, Inc.: Pittsburgh, PA, 2003.

(19) URL: http://www.emsl.pnl.gov/forms/basisform.html.

(20) Sundius, T.; Longhi, G., private communication.

(21) Pulay, P.; Fogarasi, G.; Pang, F.; Boggs, J. E. *J. Am. Chem. Soc.* **1979**, *101*, 2550–2560. Fogarasi, G.; Zhou, X.; Taylor, P. W.; Pulay, P. *J. Am. Chem. Soc.* **1992**, *114*, 8191–8201.

(22) Wilson, E. B., Jr.; Decius, J.; Cross, P. C. *Molecular Vibrations*; McGraw-Hill: New York, 1955.

(23) (a) Huang, R.; Kubelka, J.; Barber-Armstrong, W.; Silva, R. A. G. D.; Decatur, S.; Keiderling, T. A. *J. Am. Chem. Soc.* **2004**, *126*, 2346–2354. (b) Debie, E.; Bultinck, P.; Herrebout, W.; Van der Veken, B. *Phys. Chem. Chem. Phys.* **2008**, *10*, 3498–3508.

(24) (a) Hug, W.; Fedorovsky, M. *Theor. Chem. Acc.* **2008**, *119*, 113–131. (b) Fedorovsky, M.; Gerlach, H.; Hug, W. *Helv. Chim. Acta* **2009**, *92*, 1451–1465.

(25) Laux, L.; Pultz, V. M.; Abbate, S.; Havel, H. A.; Overend, J.; Moscowitz, A. *J. Am. Chem. Soc.* **1982**, *104*, 4276–4278.

(26) Abbate, S.; Castiglioni, E.; Gangemi, F.; Gangemi, R.; Longhi, G.; Ruzziconi, R.; Spizzichino, S. *J. Phys. Chem. A* **2007**, *111*, 7031–7040.

(27) Abbate, S.; Longhi, G.; Gangemi, R.; Giorgio, G.; Rosini, C. VII Convegno Nazionale, Giornate di Chimica delle Sostanze Naturali, Maratea, Italy, 2006.

(28) Pultz, V. M.; Lightner, D. A.; Moscowitz, A., private communication.

(29) Herzberg, G. *Molecular Spectra and Molecular Structure, II. Infrared and Raman Spectra of Polyatomic Molecules*; Van Nostrand Reinhold Co.: New York, 1950.

(30) (a) Polavarapu, P. L. *J. Chem. Phys.* **1987**, *87*, 6775–6775. (b) Rupprecht, A. *Mol. Phys.* **1988**, *63*, 955–958.

JP905644D